These $Pd_2X_4L_2$ complexes readily react with methanol or ethanol to provide yellow complexes that are sparingly soluble in organic solvents. As indicated in the Experimental Section, $PdCl_2[Ph_2P(o\text{-}C_6H_4C(OC_2H_5)NH)]$ has also been obtained from the reaction between H_2PdCl_4 and $PdCl_2[Ph_2P(o\text{-}C_6H_4CN)]_2$ in ethanol. The analytical and spectroscopic data (see Tables I and II) from the isolated complexes are entirely consistent with monomeric complexes containing chelating phosphine–imidate (phosphine–imino ether) ligands (**2**). Specifically, all IR spectra

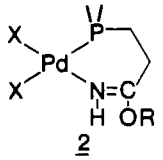

2

display strong bands in the ν(C=N) region and weak bonds in the ν(NH) region at ca. 3330 cm^{-1}, the range expected for N-coordinated imidate groups.[41] Further, as expected for cis coordination,[32,42] two ν(PdCl) bands are observed at ca. 350 and 280 cm^{-1} for the chloride-containing complexes.

Facile nucleophilic attack on organonitrile groups that are either coordinated to, or held proximate to, transition metals is well documented.[2] It has been reported, for example, that rate data from the reaction of amines with the CN group in the ligand-bridged complex $[(PPh_3)_2Pt(o\text{-}CH_2C_6H_4CN)]_2^{2+}$ indicate that the attack occurs via a $[(PPh_3)_2Pt(amine)(o\text{-}CH_2C_6H_4CN)]^+$ five-coordinated intermediate in which the nitrile group is side-on coordinated.[43] In contrast, it has been proposed that direct attack by ethanol on the end-on coordinated nitrile groups in $[(Ph_2PCHCHPPh_2)Pt(o\text{-}CH_2C_6H_4CN)]_2^+$ accounts for the rapid formation of $[(Ph_2PCHCHPPh_2)Pt(o\text{-}CH_2C_6H_4C(OC_2H_5)NH)]^+$.[44] Although the reaction may not be metal activated, it has also been reported that the uncoordinated nitrile group in $(NCCH_2PPh_2)Pd(Cl)(o\text{-}C_6H_4NMe_2)$ undergoes attack by the carbanion formed by reacting the halogen-bridged $L_2Pd_2Cl_2$ (L = o-C_6H_4NMe) with $[Ph_2PCHCN]^-$.[45]

As outlined above, most examples of metal-promoted reactions at nitrile carbons involve neutral or anionic nucleophiles and cationic complexes. The reactions reported herein clearly indicate that nitrile groups in formally neutral complexes can also be activated. Further, it is possible that the side-on coordination, shown in **1A**, activates the cyano group toward attack as suggested (vide supra) for $[(PPh_3)_2Pt(amine)(o\text{-}CH_2C_6H_4CN)]^+$[43] and proposed initially by Clark.[46]

Acknowledgment is made to the donors of the Petroleum Research Fund, administered by the American Chemical Society, and the Ball State University Faculty Research Grant program for support of this research. The assistance provided by John M. Risley and Greg L. Durst is gratefully acknowledged.

Registry No. $PdCl_2(DPPN)_2$, 96483-01-1; $PdBr_2(DPPN)_2$, 96483-02-2; $PdCl_2(DPMN)_2$ (isomer 1), 96483-03-3; $PdCl_2(DPMN)_2$ (isomer 2), 96554-68-6; $PdBr_2(DPMN)_2$ (isomer 1), 96483-04-4; $PdBr_2(DPMN)_2$ (isomer 2), 96554-69-7; $PdCl_2(DPBN)_2$, 96483-05-5; $PdBr_2(DPBN)_2$, 96483-06-6; $[PdCl_2(DPPN)]_2$, 96483-07-7; $[PdBr_2(DPPN)]_2$, 96483-08-8; $[PdCl_2(DPBN)]_2$, 96483-09-9; $[PdBr_2(DPBN)]_2$, 96483-10-2; $PdCl_2[Ph_2P(CH_2)_2C(OCH_3)NH]$, 96483-11-3; $PdBr_2[Ph_2P(CH_2)_2C(OCH_3)NH]$, 96483-12-4; $PdCl_2[Ph_2P(CH_2)_2C(OC_2H_5)NH]$, 96483-13-5; $PdCl_2[Ph_2P(o\text{-}C_6H_4C(OCH_3)NH)]$, 96483-14-6; Na_2PdCl_4, 13820-53-6; Na_2PdBr_2, 50495-13-1; DPPN, 5032-65-5; DPMN, 96483-00-0; DPBN, 34825-99-5; acrylonitrile, 107-13-1; diphenylphosphine, 829-85-6; methacrylonitrile, 126-98-7.

(41) Wada, M.; Shimohigashi, T. *Inorg. Chem.* **1976**, *15*, 954.
(42) Goodfellow, R. J.; Evans, J. G.; Goggin, P. L.; Duddell, D. A. *J. Chem. Soc. A* **1968**, 1604.
(43) Calligaro, L.; Michelin, R. A.; Uguagliati, P. *Inorg. Chim. Acta* **1983**, *76*, L83.
(44) Schwarzenbach, D.; Pinkerton, A.; Chapuis, G.; Wenger, J.; Ros, R.; Roulet, R. *Inorg. Chim. Acta* **1977**, *25*, 255.
(45) Braunstein, P.; Matt, D.; Dusausoy, Y.; Fischer, J. *Organometallics* **1983**, *2*, 1410.
(46) Clark, H. C.; Manzer, L. E. *Inorg. Chem.* **1971**, *10*, 2699.

Contribution from the Department of Chemistry, Northwestern University, Evanston, Illinois 60201, and AT&T Bell Laboratories, Murray Hill, New Jersey 07974

A Chemical, FT-IR, and EXAFS Study of the Interaction between $HFe_4(CH)(CO)_{12}$ and Partially Dehydroxylated Alumina

MARK A. DREZDZON,† CLAIRE TESSIER-YOUNGS,† CARRIE WOODCOCK,† PETER MILLER BLONSKY,† ORLANDO LEAL,† BOON-KENG TEO,*‡ ROBERT L. BURWELL, JR.,*† and DUWARD F. SHRIVER*†

Received November 16, 1984

The initial reaction of $HFe_4(CH)(CO)_{12}$ with partially dehydroxylated alumina produces $[HFe_4(C)(CO)_{12}]^-$, which is bound to the surface. Evolution of CO occurs slowly by extensive loss of CO from a small number of cluster molecules. This process leads to the coexistence of intact $[HFe_4(C)(CO)_{12}]^-$ plus an iron or iron carbide like species. In keeping with this interpretation, the supported material displays activities for the reduction of CO and the hydrogenation of benzene and product distributions that are typical of iron metal.

Introduction

The preparation of heterogeneous catalysts by the interaction of transition-metal carbonyl complexes with solid supports, especially inorganic oxides, has received widespread attention.[1-3] At low metal carbonyl loadings, the potential exists for the preparation of heterogeneous catalysts with discrete metal sites equivalent in nuclearity to the starting metal carbonyl cluster.

The chemisorption of a metal carbonyl complex on a metal oxide, however, is often much more complicated, resulting in a surface species of different nuclearity. A well-known example is the reaction of dinuclear or tetranuclear rhodium carbonyl complexes with alumina to yield $Rh_6(CO)_{16}$.[4-6] Evidence also has been presented for the formation of large osmium clusters upon

†Northwestern University.
‡AT&T Bell Laboratories.

(1) Bailey, D. C.; Langer, S. H. *Chem. Rev.* **1981**, *81*, 109–148 and references therein.
(2) Ichikawa, M. *CHEMTECH* **1982**, 674.
(3) Basset, J. M.; Choplin, A. *J. Mol. Catal.* **1983**, *21*, 95–108 and references therein.
(4) Smith, G. C.; Chojnacki, T. P.; Dasgupta, S. R.; Iwatate, K.; Watters, K. L. *Inorg. Chem.* **1975**, *14*, 1419–1421.
(5) Smith, A. K.; Hugues, F.; Theolier, A.; Basset, J. M.; Ugo, R.; Zanderighi, G. M.; Bilhou, J. L.; Bilhou-Bougnol, V.; Graydon, W. F. *Inorg. Chem.* **1979**, *18*, 3104–3112.
(6) Theolier, A.; Smith, A. K.; Leconte, M.; Basset, J. M.; Zanderighi, G. M.; Psaro, R.; Ugo, R. *J. Organomet. Chem.* **1980**, *191*, 415–424.

0020-1669/85/1324-2349$01.50/0

reaction of $Os_3(CO)_{12}$ or $Os_6(CO)_{18}$ with various metal oxides.[7]

Recently, Basset's group has found that $Fe(CO)_5$ reacts with hydrated metal oxides to form the adsorbed anionic trinuclear hydride cluster $[HFe_3(CO)_{11}]^-$.[8,9] It has been proposed that this cluster interacts with a surface metal cation through the oxygen lone pair of the bridging CO (I).[9] Infrared spectroscopic studies

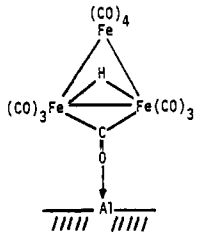

I

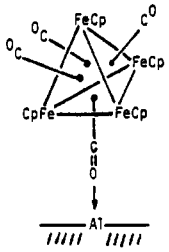

II

indicate a similar interaction for the adsorption of $[CpFe(CO)]_4$ on dehydroxylated alumina (II).[10] Homogeneous analogues of these surface species are well-known.[11]

In view of the robust nature of $HFe_4(CH)(CO)_{12}$ in superacid media and the apparent need for a minimum cluster nuclearity of four metals to activate CO,[12] the chemistry of this four-iron methyne was investigated on high surface area γ-Al_2O_3. Additionally, since $HFe_4(CH)(CO)_{12}$ is easily deprotonated in solution to form $[HFe_4(C)(CO)_{12}]^-$, the possibility also existed for carbide interaction with the support. In this study, emphasis was placed on understanding the nature of the iron carbonyl species formed upon initial interaction of the cluster with alumina and how this species changes at elevated temperatures.

Experimental Section

All operations were carried out in an atmosphere of dry nitrogen by using standard Schlenk and vacuum-line techniques.[13] Solvents were dried and distilled by using standard methods and stored under an inert atmosphere. Pentane (Aldrich, spectrophotometric grade) was stored over concentrated H_2SO_4, distilled from sodium benzophenone ketyl, and then vacuum distilled from clean sodium metal. Benzene (Aldrich, thiophene free) was distilled from potassium metal under nitrogen. FT-IR spectra were obtained on a Nicolet 7199 spectrophotometer. Gas chromatograms were recorded on a Varian Model 3700 gas chromatograph (columns: 6 ft × $^1/_8$ in. Spherocarb, 80/100 mesh at 50–300 °C for light hydrocarbons and 7 ft × $^1/_8$ in. 10% Carbowax 400/Chromosorb W at 30–50 °C for cyclohexane and benzene). Mass spectra were obtained on a Hewlett-Packard 5985 by using 70-eV electron impact.

$[PPN]_2[Fe_4(C)(CO)_{12}]$[14] and $HFe_4(CH)(CO)_{12}$[12] were prepared as described in the literature.

Synthesis of ^{13}CO-Enriched $HFe_4(CH)(^*CO)_{12}$. A 250-cm^3 Schlenk flask containing a magnetic stirring bar was charged with 2.1 g of $[PPN]_2[Fe_4(C)(CO)_{12}]$ and 50 cm^3 of freshly distilled CH_2Cl_2. The solution was degassed and placed under an atmosphere of 99% ^{13}CO. Over the next 2 weeks the ^{13}CO atmosphere was replenished twice. The CH_2Cl_2 was removed under vacuum and the tacky solid recrystallized from CH_2Cl_2/Et_2O. The enriched $[PPN]_2[Fe_4(C)(^*CO)_{12}]$ was slurried with 60 cm^3 of toluene and placed under an atmosphere of HCl gas overnight. Removal of the toluene and extraction of the residue with hexane followed by removal of the solvent under vacuum gave 0.51 g (71%) of pure $HFe_4(CH)(^*CO)_{12}$. Decomposition of a 50-mg sample in CH_2Cl_2 using $C_5H_5NHBr_3$ followed by IR spectroscopic analysis of the evolved CO showed approximately 75% enrichment in the CO ligands.

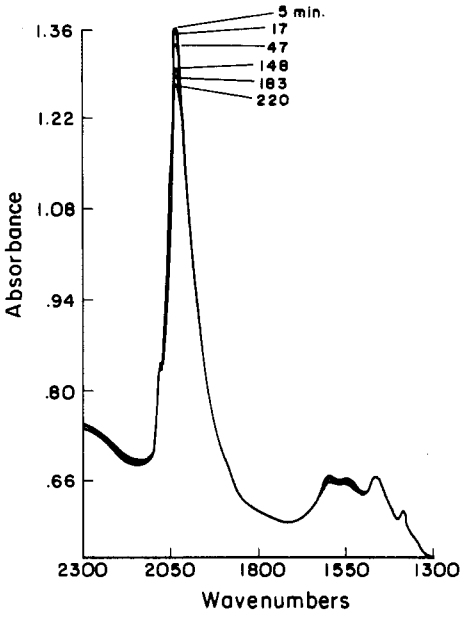

Figure 1. IR spectra of $HFe_4(CH)(CO)_{12}$ on a partially dehydroxylated alumina (PDA) film. Indicated times are after sample deposition.

Preparation of γ-Al_2O_3. High-purity γ-Al_2O_3 extrudate (American Cyanamid PHF,[10] surface area 160 m^2 g^{-1}) was crushed and sieved. The 80–100 mesh particles were washed twice with 0.1 M HNO_3 followed by washing with distilled H_2O until the washings were neutral. Fines were removed during the washing process by decantation. The alumina was then placed in a 110 °C oven overnight to remove most of the water. After being heated in air at 425 °C for 4 h, the alumina was stored in a greaseless ground-glass-stoppered bottle. The alumina was found to be inactive in the CO and benzene hydrogenation reactions described below.

FT-IR Studies of $HFe_4(CH)(CO)_{12}$ on γ-Al_2O_3. The cell for surface infrared spectroscopy of supported organometallics in an ultrapure atmosphere is described elsewhere.[10] Alumina was pressed into pellets and heated to 700 °C under flowing He. The pellet was allowed to cool to room temperature, and a pentane solution of $HFe_4(CH)(CO)_{12}$ was introduced by syringe onto the pellet under flowing He to give an average loading of 3.8% Fe. After most of the solvent had evaporated (5–10 min), the sample was placed in the infrared beam and the spectrum monitored as a function of time. Spectra were referenced to the empty cell.

EXAFS Data Collection. Extended X-ray absorption fine structure (EXAFS) fluorescence spectra of the iron K-edge were obtained on the C-2 beam line of the Cornell High Energy Synchrotron Source (CHESS).[15] The synchrotron radiation was monochromatized by a channel-cut silicon crystal (⟨220⟩ reflection) that was detuned ~50% for harmonic rejection.[16] Slits, which reside in the experimental station, were used to shape the X-ray beam size to 14 × 2 mm. An 8 cm long flow-type N_2 ionization chamber was employed to detect the monochromated beam incident on the samples. A fluorescence apparatus[17] was employed with a $Mn(acac)_2$ filter between the sample chamber and Soller slit assembly.[18] Argon was used in the fluorescence detector. The samples were loaded and sealed in rectangular glass tubes with Kapton[19] windows and stored under an inert atmosphere, to reduce the influx of air via diffusion through the window, until use. During data collection, the sample chamber was flushed with flowing helium.

EXAFS Data Analysis. The raw data were accumulated as a function of photon energy E to produce uniformly spaced intervals in k space. The photon energy was converted into a photoelectron wave vector $\mathbf{k} = [2m/\hbar^2(E - E_0)]^{1/2}$, where E_0 is the energy threshold of the iron K-edge and m is the mass of an electron. After conversion to k space (E_0 = 7119 eV (pure), 7121 eV (supported)), the data were multiplied (weighted)

(7) Collier, G.; Hunt, D. J.; Jackson, S. D.; Moyes, R. B.; Pickering, I. A.; Wells, P. B.; Simpson, A. F.; Whyman, R. *J. Catal.* **1983**, *80*, 154–171.
(8) Hugues, F.; Smith, A. K.; Ben Taarit, Y.; Basset, J. M.; Commereuc, D.; Chauvin, Y. *J. Chem. Soc., Chem. Commun.* **1980**, 68–70.
(9) Hugues, F.; Basset, J. M.; Ben Taarit, Y.; Choplin, A.; Primet, M.; Rojas, D.; Smith, A. K. *J. Am. Chem. Soc.* **1982**, *104*, 7020–7024.
(10) Tessier-Youngs, C.; Correa, F.; Pioch, D.; Burwell, R. J., Jr.; Shriver, D. F. *Organometallics* **1983**, *2*, 898–903.
(11) Shriver, D. F. *ACS Symp. Ser.* **1981**, *No. 152*, 1–18 and references therein.
(12) (a) Drezdzon, M. A.; Shriver, D. F. *J. Mol. Catal.* **1983**, *21*, 81–93. (b) Drezdzon, M. A.; Whitmire, K. H.; Bhattacharyya, A. A. Hsu, W.-L.; Nagel, C. C.; Shore, S. G.; Shriver, D. F. *J. Am. Chem. Soc.* **1982**, *104*, 5630–5633.
(13) Shriver, D. F. "The Manipulation of Air-Sensitive Compounds"; McGraw-Hill: New York, 1969.
(14) Kolis, J. W.; Holt, E. M.; Drezdzon, M.; Whitmire, K. H.; Shriver, D. F. *J. Am. Chem. Soc.* **1982**, *104*, 6134–6135.
(15) Batterman, B. W.; Ashcroft, N. W. *Science (Washington, D.C.)* **1979**, *206*, 157.
(16) Mills, D.; Pollock, V. *Rev. Sci. Instrum.* **1980**, *51*, 1664.
(17) Apparatus sold by the EXAFS Co., Seattle, WA.
(18) Stern, E. A.; Heald, S. M. *Rev. Sci. Instrum.* **1979**, *50*, 1579.
(19) E. I. du Pont de Nemours and Co., Inc., Wilmington, DE.

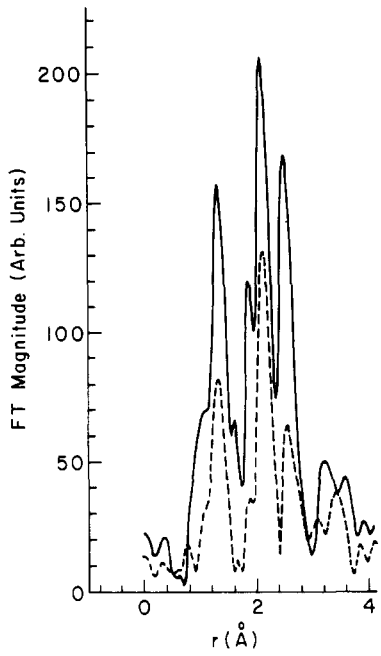

Figure 2. Fourier transforms of background-subtracted $\mathbf{k}^3\ \chi(\mathbf{k})$ vs. $\mathbf{k}$ EXAFS spectra (without phase shift correction): $HFe_4(CH)(CO)_{12}$ (dashed curve); $HFe_4(CH)(CO)_{12}$ on PDA (solid curve).

by $\mathbf{k}^3$, to compensate for amplitude attenuation, and the background removed by employing a cubic spline technique[20,21] (five sections of ca. 3 $Å^{-1}$). The EXAFS modulations were normalized by the edge jump. The data set was then Fourier transformed (cf. Figure 3),[22] and single peaks or unresolved multiple peaks were isolated with a Fourier filter and back-transformed. The filtered data in k space (cf. Figure 4, solid curves) were truncated at 3 and 14 $Å^{-1}$ and fit with a two-term single electron scattering expression (eq 1),[23] where $F(\mathbf{k})$, $\phi(\mathbf{k})$, σ, r, and $\mathbf{k}$ denote

$$\mathbf{k}^3\,\chi(\mathbf{k}) = B_a\,F_a(\mathbf{k}_a)\,\mathbf{k}_a^2[\exp(-2\sigma_a^2\mathbf{k}_a^2)]\frac{\sin\,[2\mathbf{k}_a r_a + \phi_a(\mathbf{k}_a)]}{r_a^2} + B_b\,F_b(\mathbf{k}_b)\,\mathbf{k}_b^2[\exp(-2\sigma_b^2\mathbf{k}_b^2)]\frac{\sin\,[2\mathbf{k}_b r_b + \phi_b(\mathbf{k}_b)]}{r_b^2} \quad (1)$$

amplitude, phase, Debye–Waller factor, interatomic distance, and photoelectron wave vector, respectively, and a and b represent the neighboring species to fit either the carbide carbon, carbonyl carbon, carbonyl oxygen, or iron neighboring atoms for the two shells, respectively.

Gas Evolution Studies of $HFe_4(CH)(CO)_{12}$ on γ-Al_2O_3. In a typical experiment, 700 mg of γ-Al_2O_3 was heated at 700 °C for 2 h under high vacuum, resulting in approximately 95% dehydroxylated γ-Al_2O_3 (hereafter referred to as PDA). After the PDA cooled to room temperature, 59 mg of $HFe_4(CH)(CO)_{12}$ was added to the apparatus under a nitrogen purge. The tube was reevacuated on a high-vacuum line and 5 cm^3 of pentane distilled into the apparatus. Warming slowly to 25 °C while the mixture was swirled resulted in the rapid adsorption (less than 30 s) of the $HFe_4(CH)(CO)_{12}$ onto the PDA. The pentane was removed under vacuum, and the gases evolved during adsorption were trapped on silica gel at −196 °C and then analyzed by Toepler pump measurements as well as gas chromatography. The sample was then heated to the desired temperature, and the evolved gases were similarly collected and analyzed.

Cluster Desorption Studies. The cluster was adsorbed on PDA in the above manner. After the desired period of time, the support was washed with CH_2Cl_2 (which in all cases remained colorless) and then with a CH_2Cl_2 solution of [PPN]Cl of appropriate concentration. The amount of cluster desorbed was determined by diluting the washings to a known volume and then comparing the intensity of the carbonyl bands in the IR spectrum to those obtained from both $[HFe_4(CH)(CO)_{12}]$ and $[PPN]_2[Fe_4(C)(CO)_{12}]$ solutions of known concentrations. The accuracy of these measurements is estimated to be ±5 mol %.

Batch Reactions of $HFe_4(CH)(CO)_{12}$ on PDA with H_2 or H_2/CO. In a typical experiment, 38 mg of $HFe_4(CH)(CO)_{12}$ was adsorbed on 1.00 g of PDA (corresponding to 1.5 wt % Fe) by the method previously described. After analysis of the evolved gases a measured sample of H_2 or a H_2/CO mixture was introduced, and the sample was heated to the desired temperature in a closed system containing a −196 °C silica gel trap. The product mixture was analyzed by Toepler pump measurements and gas chromatography. For samples prepared with ^{13}CO-labeled $HFe_4(CH)(CO)_{12}$, the CO/hydrocarbon product mixture was analyzed by gas-phase IR spectroscopy to determine the relative amounts of $^{13}CH_4$ and $^{12}CH_4$ and by GC-MS to determine if ^{13}C had been incorporated into the other products.

Flow Reactions of $HFe_4(CH)(CO)_{12}$ on PDA with H_2/C_6H_6. A fused silica flow reactor system was used for the benzene hydrogenation experiments. Hydrogen and helium (Matheson, ultrahigh purity) were purified by passage through traps containing silica gel, Davison grade 62, 100–120 mesh (preconditioned by heating to 475 °C for 2 h in flowing He), and then maintained at −196 °C. The flow system was checked for leaks by using a calibrated MnO/SiO_2[10] (0.3 wt % MnO) trap in place of the reactor. Both the H_2 and He feed gases were found to contain <0.04 ppm of O_2.

In a typical experiment, 100 mg of γ-Al_2O_3 was transferred to the reactor and heated to 700 °C in flowing He (approximately 90 cm^3/min) for 2 h. After the reactor was cooled to room temperature, the flow rate was increased to 200 cm^3/min, the valve stem above the reactor was removed, and 2 cm^3 of pentane was added to the reactor followed by a solution of 3.5 mg of $HFe_4(CH)(CO)_{12}$ (corresponding to 1.4 wt % Fe) in 3 cm^3 of pentane. After removal of the pentane, the flow rate was reduced to 90 cm^3/min, and the reactor was heated to the desired activation temperature for 4 h under flowing He. Under a purge of H_2 a Filtros FS-140 silica saturator upstream from the reactor was charged with benzene. The vapor saturator was maintained at 7.0 ± 0.1 °C, which corresponds to a benzene vapor pressure of 38.7 torr[24] or a H_2/C_6H_6 ratio of 19. The product gas mixture was analyzed every 20–30 min by gas chromatography via a gas-sampling valve.

Results and Discussion

Judging from extensive information on high surface area aluminas, the thermal treatment employed in the present research produces a variety of reactive surface sites: Lewis base O^{2-}, amphoteric OH^-, and Lewis acid Al^{3+}.[25] The coexistence of strong Lewis acid and base sites on these surfaces is in striking contrast with solution chemistry, where these functional groups would neutralize each other through association. Thus an alumina surface is an interesting and complex reagent. In previous studies the interaction of organometallics with the Lewis acid and Lewis base sites of alumina has been demonstrated.[3,10,26,27] In addition, the surface hydroxyl groups have been implicated as a source of reactive OH^- and a source of the oxidant H^+.[28]

The cluster $HFe_4(CH)(CO)_{12}$ is potentially susceptible to all of the surface functional groups of alumina. The CH group in this cluster is a moderately strong acid (eq 2),[29] and the CO groups are susceptible to replacement by Lewis base ligands (eq 3).[30] In

$$HFe_4(CH)(CO)_{12} + NR_3 \rightarrow [HNR_3][HFe_4(C)(CO)_{12}] \quad (2)$$

$$HFe_4(CH)(CO)_{12} + PR_3 \rightarrow HFe_4(CH)(CO)_{12-x}(PR_3)_x + x\mathrm{CO} \quad (3)$$

principle, the cluster is susceptible to oxidation by the surface

(20) Lee, P. A.; Citrin, P. H.; Eisenberger, P.; Kincaid, B. M. *Rev. Mod. Phys.* **1981**, *53*, 769.
(21) A local spline background removal routine, AT&T Bell Laboratories, Murray Hill, NJ.
(22) A local Fourier transform and Fourier filtering routine, AT&T Bell Laboratories, Murray Hill, NJ.
(23) Teo, B.-K.; Shulman, R. G.; Brown, G. S.; Meixner, A. E. *J. Am. Chem. Soc.* **1979**, *101*, 5624. Teo, B.-K.; Eisenberger, P.; Kincaid, B. M. *J. Am. Chem. Soc.* **1977**, *100*, 1735. Teo, B.-K.; Antonio, N. R.; Averill, B. A. *J. Am. Chem. Soc.* **1983**, *105*, 3751.
(24) Boublik, T.; Fried, V.; Hala, E. "The Vapor Pressures of Pure Substances"; Elsevier: New York, 1973.
(25) Peri, J. B. *J. Phys. Chem.* **1965**, *69*; 211–219, 220–230, 231–239. Lippens, B. C.; Steggerda, J. J. In "Physical and Chemical Aspects of Adsorbents and Catalysts"; Linsen, B. G., Ed.; Academic Press: New York, 1970; Chapter 4. Knözinger, H.; Ratnasamy, P.; *Catal. Rev.—Sci. Eng.* **1978**, *17*, 31–70. Tanabe, K. "Solid Acids and Bases"; Academic Press, New York, 1970.
(26) Brown, T. L. *J. Mol. Catal.* **1981**, *12*, 41–62 and references therein.
(27) Correa, F.; Nakamura, R.; Stimson, R. E.; Burwell, R. L., Jr.; Shriver, D. F. *J. Am. Chem. Soc.* **1980**, *102*, 5112.
(28) Brenner, A.; Burwell, R. L., Jr.; *J. Catal.* **1978**, *52*, 353.
(29) Tachikawa, M.; Muetterties, E. L. *J. Am. Chem. Soc.* **1980**, *102*, 4541.
(30) Muetterties, E. L.; Geerts, R. L.; Tachikawa, M.; Burch, R. R.; Sennett, M. S.; Williams, J.; Beno, M. "Abstracts of Papers", 182nd National Meeting of the American Chemical Society, New York, NY, Aug 1981; American Chemical Society: Washington, DC, 1981; INOR 89.

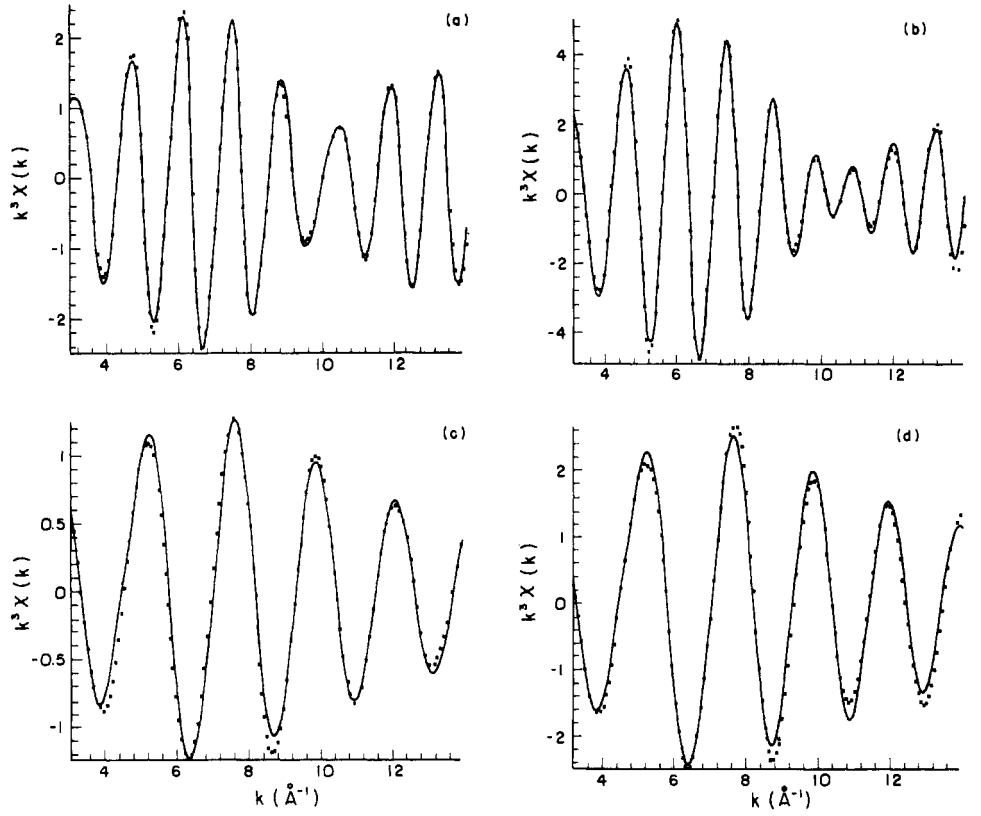

Figure 3. Best fit nonlinear least-squares curves (dots) of Fourier filtered $\mathbf{k}^3\chi(\mathbf{k})$ vs. k EXAFS spectra (solid curve): (a) $HFe_4(CH)(CO)_{12}$ Fe–Fe/Fe–O (filtering window 1.7–3.2 Å); (b) $HFe_4(CH)(CO)_{12}/Al_2O_3$ Fe–Fe/Fe–O (filtering window 1.7–3.2 Å); (c) $HFe_4(CH)(CO)_{12}$ Fe–C(CO)/Fe–C (filtering window 0.8–1.8 Å); (d) $HFe_4(CH)(CO)_{12}/Al_2O_3$ Fe–C(CO)/Fe–C (filtering window 0.8–1.8 Å).

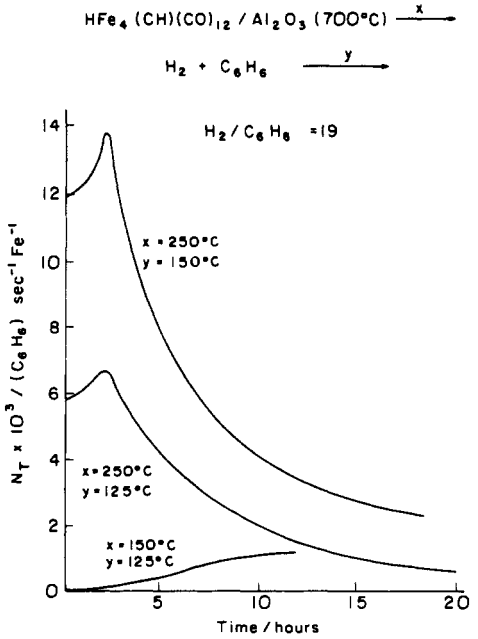

Figure 4. Turnover number vs. time for the hydrogenation of benzene over $HFe_4(CH)(CO)_{12}$ on PDA. The cluster loading corresponds to 1.5 wt % Fe on Al_2O_3.

protons; however, this seems unlikely, at room temperature, in view of the low rate of reaction between $HFe_4(CH)(CO)_{12}$ and the superacid HSO_3CF_3.[12a]

Since the most powerful structural tools of molecular chemistry, X-ray diffraction and high-resolution NMR, are not available to characterize surface species, other methods must be used. In the present research we have employed infrared spectroscopy, extended X-ray absorption fine structure spectroscopy, and a variety of chemical tests from which we infer the nature of the surface organometallic products.

FT-IR, Gas Evolution, and Cluster Desorption Studies. FT-IR spectroscopic studies of $HFe_4(CH)(CO)_{12}$ adsorbed on PDA at room temperature reveal a shift of the main CO stretching band to 2026 cm^{-1} (Figure 1). This frequency is intermediate between the main band in the solution spectrum of the neutral $HFe_4(CH)(CO)_{12}$, 2053 cm^{-1}, and that of the anion $[HFe_4(C)(CO)_{12}]^-$, 2005 cm^{-1}.[12] A likely mode of interaction with the surface is deprotonation of the cluster.[25] Some proposed structures for the resulting surface-supported complex are shown in III–VI. First,

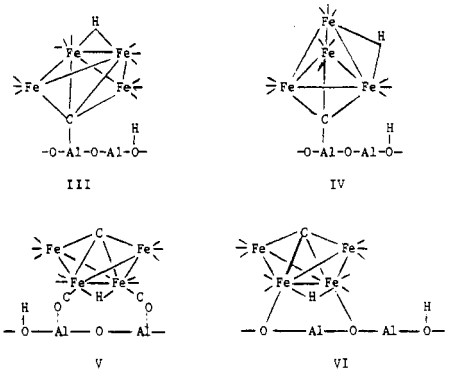

as shown by III, the cluster carbide ligand may be deprotonated by a Lewis base site and then coordinated by a Lewis acid site as the intact butterfly cluster. This coordination may also be accompanied by a rearrangement of the metal framework to a tetrahedron as shown by IV. This type of metal framework rearrangement has been observed previously in the reaction of $[Fe_4(C)(CO)_{12}]^{2-}$ with strong electrophiles (eq 4).[31] Interaction

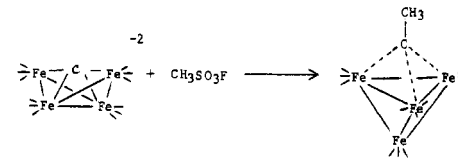

Table I. Effect of Temperature upon the Moles of CO Evolved per Mole of Cluster for the Interaction of $HFe_4(CH)(CO)_{12}$ with Partially Dehydroxylated γ-Al_2O_3[a]

	mol of CO lost/mol of cluster		
T/°C	4 h	8 h	48 h
25	0.34	0.46	0.81
75	2.24	2.67	
125	4.90	5.36	
175	6.78	6.94	

[a] Yields are cumulative.

of the cluster with the surface via carbonyl ligands, as shown by V, would lead to a decrease in stretching frequency for the carbonyl ligands bound to the surface and an increase in frequency for the remaining carbonyl ligands. This effect is clearly observed with $[HFe_3(CO)_{11}]^-$ supported on γ-Al_2O_3. The cluster exhibits absorptions at 2073 (w), 2008 (s), 2000 (s), and 1709 (m) cm^{-1} (C_6H_6 solvent) compared to ν(CO) bands for the adsorbed cluster at 2082 (w), 2020 (s), 2008 (s), and 1598 (m) cm^{-1}, where the lowest frequency band is thought to originate from a C- and O-bonded carbonyl.[9] In the present study, structure V is ruled out on the basis of the IR data, which indicate no lowered ν(CO) bands. The replacement of CO ligands by Lewis base sites (VI) has been observed for the interaction of $Mo(CO)_6$ with alumina, yielding $Mo(CO)_3$(ads).[26] However, in the present study, quantitative measurements of evolved gases show that the initial interaction of $HFe_4(CH)(CO)_{12}$ with PDA results in the loss of only 0.1 mol of CO/mol of cluster, thus ruling out VI as a major mode of interaction. Displacement of CO ligands by the surface, however, may be important at later stages of reaction where cluster breakup occurs as discussed below. In this investigation we cannot definitively choose between structures III and IV.

If the adsorbed cluster is allowed to stand under vacuum at room temperature for 8 h, a total of 0.46 mol of CO/mol of $HFe_4(CH)(CO)_{12}$ (including that lost upon adsorption) is evolved (Table I). This value is in good agreement with results obtained under similar conditions by FT-IR spectroscopic studies, which show a 5% loss in integrated intensity for the CO stretching region of the adsorbed cluster (Figure 1). Even after 2 days, less than 1 mol of CO/mol of cluster is lost, indicating the adsorbed cluster is fairly stable under vacuum at room temperature.

The evolved CO appears to originate from a small percentage of the cluster molecules as indicated by the rapid desorption of the cluster on washing with excess [PPN]Cl in CH_2Cl_2. The cluster is recovered in 95% yield if the support is washed immediately after adsorption. Additionally, 85% of the cluster is recovered 12 h after adsorption whereas only 65% is recovered after 40 h. In all cases the cluster is recovered as a mixture of [PPN][$HFe_4(C)(CO)_{12}$] and [PPN]$_2$[$Fe_4(C)(CO)_{12}$] as determined by IR spectroscopy. However, if only 1 equiv of [PPN]Cl is employed and the contact time minimized, then 20% of the cluster can be recovered as pure [PPN][$HFe_4(C)(CO)_{12}$]. These experiments indicate that the large majority of cluster molecules maintain their structural integrity upon initial interaction with the alumina surface. Also, the cluster appears to be initially desorbed as the monoanion, which undergoes further reaction with the surface to form the dianionic species (eq 5).

$$HFe_4(CH)(CO)_{12}(ads) \xrightarrow{[PPN]Cl} [PPN][HFe_4(C)(CO)_{12}] \xrightarrow[surface]{[PPN]Cl} [PPN]_2[Fe_4(C)(CO)_{12}] \quad (5)$$

Further experiments show that exposure of the adsorbed cluster to atmospheric oxygen results in an instantaneous color change from dark brown to rust orange. This demonstrates the extreme air sensitivity of this supported metal carbonyl. Additionally, when the adsorbed cluster is heated under vacuum, increasing amounts of CO are lost as the temperature is increased (Table I). Most of the CO loss at a particular temperature occurs during the first 4 h. Again, analysis of the evolved gases by GC indicates that only CO is evolved; no H_2 or hydrocarbons are detected.

Table II. Best Fit Nonlinear Least-Squares Refined Interatomic Distances r (Å), Debye–Waller Factors σ (Å), Energy Threshold Differences ΔE_0 (eV), Edge Position Energies E_0 (eV), and r Values Obtained from Single-Crystal X-ray Diffraction Studies

	EXAFS				X-ray	
term	E_0	ΔE_0	σ	r	r[c]	% error
Fe–Fe[a]	7119	−8.13	0.048	2.57	2.616 (2)	1.8
Fe–O(CO)[a]	7119	−7.47	0.051	3.01	2.95 (2)	2.0
Fe–C(CO)[a]	7119	8.80	0.024	1.75	1.804 (2)	3.0
Fe–C[a]	7119	−8.67	0.027	1.84	1.911 (2)	3.7
Fe–Fe[b]	7121	−4.43	0.100	2.62		
Fe–O(CO)[b]	7121	−9.26	0.000	3.01		
Fe–C(CO)[b]	7121	9.26	0.055	1.74		
Fe–C[b]	7121	−9.16	0.034	1.80		

[a] Pure $HFe_4(CH)(CO)_{12}$. [b] Supported $HFe_4(CH)(CO)_{12}$. [c] Reference 32.

To further understand the nature of the cluster–support interaction, a range of cluster loadings were examined. The maximum loading was 3.8 wt % Fe, which corresponds to an average separation of 4 Å between carbonyl oxygens of different clusters, whereas the minimum loading examined was 1.4 wt % Fe, resulting in an average separation of 12 Å between the peripheries of adjacent clusters. Carbon monoxide evolution data on these systems were identical with those reported in Table I, which indicates that the distance between clusters has no effect on the cluster–surface interaction.

EXAFS of $HFe_4(CH)(CO)_{12}$ and PDA-Bound $HFe_4(CH)(CO)_{12}$. Fourier transforms of the $\mathbf{k}^3\chi(\mathbf{k})$ vs. $\mathbf{k}$ data of $HFe_4(CH)(CO)_{12}$ and PDA-bound $HFe_4(CH)(CO)_{12}$, depicted as solid and dashed curves, respectively, in Figure 2, show three distinct peaks. The peaks at successively larger r are attributed to the Fe–C(CO,C), Fe–Fe, and Fe–O(CO) distances. The filtered data (Figure 3) were fit with the two-term model (eq 1) for each of the Fe–C and Fe–Fe/Fe–O peaks. The best fit distances are shown in Table II. Also included are results obtained by single-crystal X-ray crystallography.[32] The average Fe–Fe and Fe–O distances determined by EXAFS agree to within 2% of those reported. The Fe–C distances for both the carbonyls and carbide are less accurate, owing to the wide range of crystallographic distances (1.777 (2)–1.952 (2) Å).[32] No significant changes are observed in bond distances when the cluster is adsorbed on PDA. No changes are seen in the Fe–C or Fe–O distances of the carbonyl groups, and the small increase in the Fe–Fe distance is negligible within experimental error.

As is evident from Figure 2, the relative peak heights of the Fourier transform of the EXAFS spectra of $HFe_4(CH)(CO)_{12}$ do not change drastically upon adsorption on PDA. This observation, coupled with the similar distances determined by EXAFS for the pure and PDA-bound $HFe_4(CH)(CO)_{12}$ (cf. Table II), suggests that the cluster does not undergo drastic local structural changes upon adsorption. In other words, the heavy-atom (non-hydrogen) skeletons of the majority of the clusters, after deprotonation, remain more or less intact after interaction with the surface. However, small amounts of iron metal or iron carbide are indicated by the enhanced peak at 2.62 Å. The iron–iron distances for metallic iron and Cementite (FeC) were determined to be approximately 2.6 Å in this study and therefore are indistinguishable from the Fe–Fe distance of $HFe_4(CH)(CO)_{12}$ by EXAFS.

The best fit Debye–Waller factors (σ) for each major feature in the radial distribution function (Figure 3) are tabulated in Table II. With the exception of the Fe–O term, which is affected by the focusing effect, the σ values increase significantly upon adsorption.[33,34] These increases signal a significantly higher degree

(31) Holt, E. M.; Whitmire, K. H.; Shriver, D. F. *J. Am. Chem. Soc.* **1982**, *104*, 5621–5626.

(32) Beno, M. A.; Williams, J. M.; Tachikawa, M.; Muetterties, E. L. *J. Am. Chem. Soc.* **1981**, *103*, 1485–1492.

Table III. Product Yields Obtained from the Reaction of $HFe_4(CH)(CO)_{12}$ on PDA with H_2 and Then with H_2/CO Mixtures[a]

	cycle 1[b] mol of gas/mol of complex	cycle 2[c] mol of gas/mol of complex	cycle 3[d] mol of gas/mol of complex
CO_2	0.00	0.01	0.78
CH_4	4.34	1.76	1.21
C_2H_6	0.69	0.26	0.35
C_3H_8	0.48	0.19	0.28
C_4H_{10}	0.03	trace	0.01
H_2 consumed	22.7	7.7	6.8
CO consumed		5.6	6.6
H_2 in products	20.1	7.9	7.4
CO in products	7.3	2.9	3.6
H_2 accounted for	89%	103%	108%
CO accounted for		52%	55%

[a] The cycles were run sequentially on the same sample. Prior to each cycle the reactor was cooled to room temperature and charged with the indicated gases. The cluster loading corresponds to 1.5 wt % Fe on Al_2O_3. [b] 575 torr H_2, 175 °C, 24 h. [c] 400 torr H_2, 119 torr CO, 175 °C, 24 h. [d] 471 torr H_2, 145 torr CO, 175 °C, 24 h.

of structural disorder, arising from nonequivalent bond distances, upon adsorption.

Batch Reactions of PDA-Supported $HFe_4(CH)(CO)_{12}$. When PDA-supported $HFe_4(CH)(CO)_{12}$ is heated to temperatures less than 150 °C for 24 h in a closed system under either a H_2 or a H_2/CO atmosphere, no H_2 is consumed and the amount of CO produced is the same as that produced when the supported cluster is heated under vacuum (Table I). Similarly, the IR spectra of the supported cluster at room temperature are identical under vacuum, H_2, and CO. These results further stress the strength of the cluster–support interaction at room temperature.

When the $HFe_4(CH)(CO)_{12}$/PDA system is heated to 175 °C for 24 h in a static reactor under H_2, C_1–C_4 saturated hydrocarbons are produced. In the absence of PDA, heating either $HFe_4(CH)(CO)_{12}$ or $[PPN][HFe_4(C)(CO)_{12}]$ to 175 °C under H_2 for 24 h leads to the evolution of 6–10 equiv of CO and less than 0.5 equiv of methane. Similarly, heating a THF solution of $[PPN][HFe_4(C)(CO)_{12}]$ to 55 °C under H_2 for 24 h results in the liberation of ca. 2 equiv of CO and no detectable hydrocarbon formation.

The first column of Table III lists the results obtained for the reaction of H_2 with a material corresponding to 1.5 wt % Fe on PDA. As shown in Table III, 89% of the H_2 consumed in the reaction is accounted for by assuming that the product formation follows eq 6, and the total amount of carbon in the products agrees

$$n\mathrm{CO} + (2n + 1)\mathrm{H_2} \rightarrow \mathrm{C}_n\mathrm{H}_{2n+2} + n\mathrm{H_2O} \qquad (6)$$

well with the amount of carbon that would have been lost, in the form of CO, if the system was heated under vacuum at 175 °C (cf. Table I). The most important feature of the distribution of gaseous products shown in Table III is the rapid decrease in hydrocarbon yield with carbon number, similar to that found in conventional Fischer–Tropsch catalysts.[35] This indicates that the hydrogenation reaction is most likely occurring on sintered iron or iron carbide particles. Analogous behavior has been noted for the reaction of highly dispersed $Fe_3(CO)_{12}$ on PDA (0.82 wt % Fe) with H_2 and CO at 270 °C, where iron particles on the order of 200–500 Å are produced.[36]

After reaction of a particular sample with H_2 at 175 °C for 24 h, the material was further treated with a mixture of H_2 and CO under the same conditions. Results of these consecutive cycles are listed in the last two columns of Table III. Again, the product distribution suggests the reaction is occurring on sintered iron or iron carbide particles. Also, the yield of products decreases with time, indicating a deactivation of the material, which may be due to the formation of an inactive carbonaceous layer. The appearance of CO_2 in the product mixture after extended periods of reaction most probably arises from the water-gas shift reaction ($CO + H_2O = CO_2 + H_2$). When the sequence depicted in Table III is carried out at 200 °C a slight but uniform increase in the hydrocarbon products occurs.

To understand further the nature of the cluster–support interaction, the ^{13}C-labeled cluster $HFe_4(CH)(^{13}CO)_{12}$ was adsorbed on PDA and reacted with H_2. Gas-phase IR spectroscopic studies of the product gas mixture reveal that only 80% of the CH_4 produced originates from the CO ligands, indicating that the carbide ligand must supply 20% of the carbon used in hydrocarbon production. This is confirmed by mass spectroscopic studies that show an upward shift of 2–3 mass units for the C_3 and C_4 products. Additionally, incorporation of the carbide ligand into the hydrocarbon products may suggest that a cluster reorganization process occurs on the surface.

Flow Reactions of $HFe_4(CH)(CO)_{12}$ on PDA with H_2/C_6H_6. Due to the thermal instability of the supported cluster, a less thermally demanding reaction was required to probe the reactivity of this system. The benzene hydrogenation reaction was chosen because it has been reported to occur at lower temperatures and is thought to require an ensemble of metal atoms.[37,38] Figure 4 illustrates the results obtained when the hydrogenation of benzene is carried out in the flow reactor containing $HFe_4(CH)(CO)_{12}$ on PDA. After cluster adsorption, the catalyst is activated by heating under flowing He for 4 h at 150 °C (bottom curve) or 250 °C (top two curves). Reaction with a 19:1 molar ratio of $H_2:C_6H_6$ is then carried out at 125 °C (bottom two curves) or 150 °C (top curve). Cyclohexane is the only product detected in all cases.

The catalysts activated at 250 °C show behavior similar to that seen on conventionally prepared 10% Fe on Al_2O_3 catalysts,[39,40] which indicates that the harsh conditions used to activate the catalyst caused sintering of the supported clusters into iron particles. However, when the activation process is carried out at 150 °C (lower curve), the initial catalytic activity is very low and only slowly increases during the first 12 h. At this time the activity levels off at a turnover frequency comparable to those of the catalysts activated at 250 °C. Plausible explanations for this behavior include the following: (1) The activation temperature of 150 °C may not have been high enough to drive CO off the adsorbed cluster; therefore, the activity increases due to the slow loss of additional CO as the reaction progresses. (2) A cluster reorganization process, which would be much slower at this lower temperature, may be occurring on the surface.

Conclusions

The initial reaction of $HFe_4(CH)(CO)_{12}$ with partially dehydroxylated γ-alumina (PDA) occurs with very little CO evolution and a 27-cm^{-1} shift of the strongest CO stretching frequency to lower energy. These data indicate the formation of a bound anionic cluster, $[HFe_4(C)(CO)_{12}]^-$. About 95% of the cluster can be eluted as $[PPN][HFe_4(C)(CO)_{12}]$. Upon standing, the infrared absorptions in the CO stretching region slowly diminish in intensity, CO is slowly evolved, and the amount of $[PPN][HFe_4(C)(CO)_{12}]$ that can be eluted from the surface diminishes. These data indicate that the predominant mode of decomposition for the adsorbed species, $[HFe_4(C)(CO)_{12}]^-$, is not uniform CO loss from each cluster. Apparently, the loss of the first CO from a cluster facilitates subsequent decomposition (eq 7). In agreement with this observation, EXAFS data collected after the sample had aged for 4 days indicate the presence of intact cluster plus a small amount of iron metal or iron carbide. Homogeneous analogues

(33) Teo, B.-K. In "EXAFS Spectroscopy"; Teo, B.-K., Joy, D. C., Eds.; Plenum Press: New York, 1983; p 13.
(34) Via, G. H.; Sinfelt, J. H.; Lytle, F. W. *Catal. Rev.—Sci. Eng.* **1984**, *26*, 81.
(35) Henrici-Olivé, G.; Olivé, S. *Angew. Chem., Int. Ed. Engl.* **1976**, *15*, 136–141 and references therein.
(36) Commereuc, D.; Chauvin, Y.; Hugues, F.; Basset, J. M.; Olivier, D. *J. Chem. Soc., Chem. Commun.* **1980**, 154–155.
(37) Puddu, S.; Ponec, V. *Recl. Trav. Chim. Pays-Bas* **1976**, *95*, 255–284.
(38) Martin, G. A.; Dalmon, J. A. *J. Catal.* **1982**, *75*, 233–242.
(39) Badilla-Ohlbaum, R.; Neuburg, H. J.; Graydon, W. F.; Phillips, M. J. *J. Catal.* **1977**, *47*, 273–279.
(40) Yoon, K. J.; Vannice, M. A. *J. Catal.* **1983**, *82*, 457–468.

$$x\mathrm{HFe_4(CH)(CO)_{12}(ads)} \xrightarrow[-\mathrm{CO}]{\text{slow}} y\mathrm{HFe_4(CH)(CO)_{12}(ads)} + (x-y)\mathrm{HFe_4(CH)(CO)_{11}(ads)} \xrightarrow[-\mathrm{CO}]{\text{fast}} y\mathrm{HFe_4(CH)(CO)_{12}(ads)} + \mathrm{Fe(ads)\ (or\ FeC(ads))} \quad (7)$$

for the activation of metal carbonyls by attached ligands are known.[41]

To further explore the nature of the surface carbonyl species, the reactions of CO/H_2 and of benzene/H_2 over the supported cluster were investigated. In a batch reactor, the CO/H_2 mixture did not produce reduction products of CO below 175 °C, and at that temperature the product distribution appeared to be similar to that produced in conventional Fischer-Tropsch chemistry. Apparently at these high temperatures, the surface species closely approximates bulk iron or iron carbide. The surface species have activity for benzene hydrogenation at lower temperatures, but cyclohexane was the only significant product, and therefore no evidence exists from this experiment for catalytic ensembles that differ from the bulk metal in catalytic properties.

Acknowledgment. We appreciate the support of DOE (Grant DE-AC02-83ER13104) for studies on the characterization of surface species and the Gas Research Institute (Grant 5082-260-0693) for studies on the reactivity of the adsorbed clusters. P.M.B. thanks Paula Bogdan and Andrew Lang for assistance in collecting EXAFS data. D.F.S. thanks the John Simon Guggenheim Foundation for a fellowship.

Registry No. $HFe_4(CH)(CO)_{12}$, 74792-06-6; $[HFe_4(C)(CO)_{12}]^-$, 74792-02-2; Al_2O_3, 1344-28-1; CO, 630-08-0.

(41) Butts, S. B.; Strauss, S. H.; Holt, E. M.; Stimson, R. E.; Alcock, N. W.; Shriver, D. F. *J. Am. Chem. Soc.* **1980**, *102*, 5093. Richmond, T. G.; Basolo, F.; Shriver, D. F. *Inorg. Chem.* **1982**, *21*, 1272.

Contribution from the Departments of Chemistry, Wayne State University, Detroit, Michigan 48202, and Martin-Luther University, 402 Halle(s), G.D.R.

Synthetic and Spectroscopic Studies into the Mechanism of the $[Pt(PR_3)_4]/R_2P(S)H$ Reaction. Formation and Structure of the Novel Diplatinum(II) Dihydride Complex $[Pt_2(H)_2(P\text{-}t\text{-}Bu_3)_2(\mu\text{-}SPPh_2)_2]$

A. F. M. M. RAHMAN,[1a] C. CECCARELLI,[1a] J. P. OLIVER,*[1a] B. MESSBAUER,[1b] H. MEYER,[1b] and B. WALTHER*[1b,2]

Received May 25, 1984

The reaction of $[Pt(PR'_3)_4]$ (R' = alkyl, phenyl) with $Ph_2P(S)H$ yields the diplatinum(I) complexes $[Pt_2(PR'_3)_2(\mu\text{-}SPPh_2)_2]$. The reaction proceeds via the isolable intermediate $[PtH(PR'_3)_2\{P(S)Ph_2\}]$ which exists in solution as a mixture of the trans and cis isomers. Both isomers lose one phosphine ligand at higher temperatures, yielding coordinately and electronically unsaturated species that form the final diplatinum(I) complexes. The intermediates have been characterized by NMR spectroscopy and the results discussed in comparison to the reaction of $[Pt(PR'_3)_4]$ with $Ph_2P(O)H$. $[Pt(P\text{-}t\text{-}Bu_3)_2]$ and $Ph_2P(S)H$ react unexpectedly to give the novel diplatinum(II) complex $[Pt_2(H)_2(P\text{-}t\text{-}Bu_3)_2(\mu\text{-}SPPh_2)_2]$ which has been characterized by ^{31}P and ^1H NMR spectroscopy and by a single-crystal structure determination. It crystallizes in the monoclinic system, space group $C2/c$, with cell dimensions of a = 18.063 (1) Å, b = 16.572 (1) Å, c = 17.318 (1) Å, β = 92.240 (5)°, V = 5180.1 (6) Å^3, and Z = 4. Full-matrix least-squares refinement on 2362 data gave R = 3.5% and R_w = 4.6%. The structure determination has shown that the platinum(II) atoms have square-planar geometry surrounded by bridging S and P atoms and terminal P and H atoms and that the Pt-S-P(1)'-Pt'-S'-P(1) unit is in a boat conformation. Each of the Pt-S-P(1)'-Pt' units is planar. The planar atoms in the dimer are 3.620 (1) Å apart, ruling out the possibility of metal-metal interactions. The other distances around Pt are as follows: Pt-S = 2.451 (3) Å, Pt-P(1)(bridge) = 2.285 (3) Å, Pt-P(2)(terminal) = 2.330 (3) Å, and Pt-H(66) = 1.42 Å.

Introduction

Secondary phosphine chalcogenides, $R_2P(E)H$ (E = O, S, Se), form different types of derivatives when reacted with (tertiary phosphine)platinum(0) complexes, $[Pt(PR'_3)_4]$. Thus, if E = O mononuclear complexes containing the uninegative bidentate hydrogen-bridged ligand $(Ph_2PO\cdots H\cdots OPPh_2)^-$ are formed according to eq 1.[3] If, however, E = S or Se, bis(chalcogenophosphinito)-bridged diplatinum(I) complexes result as outlined in eq 2.[4]

$$[Pt(PR'_3)_4] + 2R_2P(O)H \rightarrow [PtH(PR'_3)\{R_2PO)_2H\}] + 3PR'_3 \quad (1)$$

$$2[Pt(PR'_3)_4] + 2R_2P(E)H \xrightarrow{E = S, Se} [Pt_2(PR'_3)_2(\mu\text{-}EPR_2)_2] + 6PR'_3 + H_2 \quad (2)$$

The first reaction involves an oxidative-addition step to form $[Pt^{II}H(PR'_3)_2\{P(O)R_2\}]$ which (either in a conserted or subsequent step) substitutes $R_2P(O)H$ for one PR'_3 ligand. The driving force for this latter step is the formation of the strong hydrogen bond. Reaction 2 is unique in that treatment of $[Pt(PR'_3)_4]$ with a protic acid yields a diplatinum(I) complex. Therefore, we have undertaken a study to elucidate the mechanism of this reaction. This paper reports attempts to characterize the key intermediate of reaction 2, $[PtH(PR'_3)_2\{P(S)R_2\}]$. In the course of this study we unexpectedly found that treatment of $[Pt(P\text{-}t\text{-}Bu_3)_2]$ with $Ph_2P(S)H$ yields the novel diplatinum(II) dihydride complex, $[Pt_2(H)_2(P\text{-}t\text{-}Bu_3)_2(\mu\text{-}SPPh_2)_2]$, whose structure has been established by single-crystal X-ray analysis.

Experimental Section

General Procedures. All reactions were carried out anaerobically by using conventional Schlenk techniques. Solvents were dried, deoxygenated, and distilled just prior to use. Starting materials were prepared according to literature procedures: $[Pt(PMePh_2)_4]$,[5] $[Pt(P\text{-}t\text{-}Bu_3)_2]$,[6] $Ph_2P(S)H$.[7] Details of the NMR measurements are given elsewhere.[8]

***trans*/*cis*-[Pt(H)(PMePh$_2$)$_2${P(S)Ph$_2$}] (1a/1b).** A 218-mg (1 mmol) sample of solid $Ph_2P(S)H$ was added to a solution of 995 mg (1 mmol) of $[Pt(PMePh_2)_4]$ in 40 mL of toluene at −20 °C. After 4 h of stirring at −20 °C, the solution was filtered into 70 mL of *n*-pentane that had been cooled to −60 °C. The precipitate was filtered off at −70 °C, washed with 40 mL of diethyl ether precooled to −60 °C, and dried 8 h

(1) (a) Wayne State University. (b) Martin-Luther University.
(2) Secondary Phosphine Chalcogenides. 9. Part 8: Zschunke, A.; Meyer, H.; Heidlas, I.; Messbauer, B.; Walther, B.; Schadler, H.-D.; Thomas, B. *Z. Anorg. Allg. Chem.* **1983**, *504*, 117.
(3) Beaulieu, W. B.; Rauchfuss, T. B.; Roundhill, D. M. *Inorg. Chem.* **1975**, *14*, 1732.
(4) Walther, B.; Messbauer, B.; Meyer, H. *Inorg. Chim. Acta* **1979**, *37*, L525.
(5) Mukhedkar, A. J.; Green, M.; Stone, F. G. A. *J. Chem. Soc. A* **1969**, 3023.
(6) Goel, R. G.; Ogini, W. P.; Srivastava, R. C., *J. Organomet. Chem.* **1981**, *214*, 405.
(7) Peters, G., *J. Org. Chem.* **1962**, *27*, 2198.
(8) Messbauer, B.; Meyer, H.; Walther, B.; Heeg, M. J.; Rahman, A. F. M. M.; Oliver, J. P. *Inorg. Chem.* **1983**, *22*, 272.

0020-1669/85/1324-2355$01.50/0